

RECENT ADVANCES IN HIGH-RESOLUTION LAGRANGIAN TRANSPORT MODELING

Jennifer Hegarty*, Thomas Nehrkorn, Janusz Eluszkiewicz, John Henderson, Mark Leidner and
Marikate Mountain
Atmospheric and Environmental Research, Lexington, MA, USA

Roland Draxler, Ariel Stein and Fong Ngan
NOAA Air Resources Laboratory, College Park, MD, USA

Jerome Brioude
Cooperative Institute for Research in Environmental Sciences, University of Colorado, Boulder, CO, USA

Kathryn McKain and Steven Wofsy
Harvard University, Cambridge, MA USA

Philip DeCola and Taylor Jones
Sigma Space Corporation, Lanham, MD, USA

Arlyn Andrews
NOAA Earth Systems Research Laboratory, Global Monitoring Division, Boulder, CO, USA

1. INTRODUCTION

The accuracy of air quality simulations reflects the fidelity of the atmospheric transport model employed that in turn is highly dependent on the accuracy of the meteorological input data. In this work we present some recent advances in Lagrangian transport modeling obtained through Lagrangian particle dispersion model (LPDM) simulations driven by various combinations of meteorological inputs. First we applied controlled tracer release experiments to evaluate the Hybrid Single Particle Lagrangian Integrated Trajectory Model (HYSPLIT), Stochastic Time-Inverted Lagrangian Transport (STILT) and FLEXible PARTicle (FLEXPART) LPDMs driven by identical meteorological fields from the North American Regional Reanalysis (NARR, Mesinger et al. 2006)) and Weather Research and Forecasting (WRF) model (Skamarock and Klemp, 2008). A rigorous statistical evaluation was applied to the simulations to identify each LPDM's sensitivity to the various meteorological inputs. Next, we describe the application of STILT driven by WRF inputs (WRF-STILT) to greenhouse gas (GHG) simulations in urban areas including Salt Lake City and Boston. These studies included an analysis of

the improvements achievable by increasing the spatial resolution employing advanced urban parameterizations in WRF. These urban GHG studies also include an ongoing investigation into the feasibility of incorporating advanced instrumentation such as Mini Micro-Pulse LiDARs to evaluate and potentially improve the fidelity of the WRF simulations.

2. LPDM INTERCOMPARISON

Three state-of-the-science LPDMs, HYSPLIT (Draxler and Hess 1998), STILT (Lin et al. 2003), and FLEXPART (Stohl et al. 1998, 2005) were evaluated using measurements from two historical controlled tracer release experiments. A complete description of the study and the findings summarized here are provided in Hegarty et al. (*in press, J. Appl. Meteorol. Clim*). The Cross-Appalachian Tracer Experiments (CAPTEX, Ferber et al. 1996) took place in September and October of 1983 and included six 3-hour perfluoromonomethylcyclohexane (PMCH) releases from Dayton, OH (CAPTEX-1 through -4) and Sudbury, ON Canada (CAPTEX-5 and -7) and measurements at 84 sites 300 to 800 km from the release sites. The Across North America Tracer Experiment (ANATEX, Draxler and Heffter 1989) took place in January - March of 1987 and featured 3-hour releases of perfluorotrimethylcyclohexane (PTCH) from Glasgow, MT (GGW) and perfluorodimethylcyclohexane

*Corresponding author: Jennifer Hegarty, Atmospheric and Environmental Research, 131 Hartwell Avenue, Lexington, MA 02421; e-mail: jhegarty@aer.com, phone:781-761-2377, fax: 781-761-2299

(PDCH) from Saint Cloud, MN (STC) every 2.5 days and measurements at 75 sites located throughout southeastern Canada and the eastern US. Individual forward-in-time concentration simulations were conducted for each of the CAPTEX releases while a single simulation for each location including all of the releases for each location from 5 -15 January was conducted for ANATEX. Only a subset of the ANATEX data was used so that there would be about the same number of observations for both the ANATEX and CAPTEX experiments included in the statistical evaluations.

The LPDM simulations were driven by hourly 10 km meteorological fields created by the Advanced Research WRF (ARW) model, version 3.2.1. Additional HYSPLIT and STILT runs were conducted using only 3-hourly 32 km NARR fields to provide a benchmark to the WRF driven simulations; however, these additional runs were not possible for FLEXPART since the version used was specifically designed to use WRF inputs.

The initial and boundary conditions for WRF were provided to WRF in its outer 30 km nest by NARR. The WRF simulations were restarted each day at 0000 UTC and 3-D grid nudging of temperature and moisture and wind fields to NARR was applied above the planetary boundary layer (PBL) in both domains every 3 hours. Sensitivity runs were performed with two different nudging configurations for the PBL, one with PBL wind nudging turned on ($pb=1$) and one with it turned off ($pb=0$). WRF can produce outputs specifically implemented for the benefit of transport simulations (Nehrkorn et al. 2010) and these include time-averaged mass-coupled horizontal and vertical velocities, to improve mass conservation and the representation of wind variability, and time-averaged mass fluxes from the WRF moist convective parameterization scheme. LPDM sensitivity studies were conducted in which the models were driven with either the time-averaged fields (*avrg*) or the instantaneous fields (*inst*).

The simulations were evaluated using four statistical parameters selected to represent well-defined evaluation categories and these were: the correlation coefficient (R), the fractional (normalized) bias (FB), the figure-of-merit in space (FMS) to measure the modeled-observed tracer plume overlap (defined here with a tracer concentration threshold value of 0 pg m^{-3}), and the Kolmogorov-Smirnov parameter (KSP) to represent the similarity between modeled and observed concentration distributions (Mosca et al. 1998). The four parameters were combined to

produce an overall statistical rank following Draxler (2006) as shown in (1).

$$\text{Rank} = R^2 + 1 - |FB/2| + FMS/100 + (1 - KSP/100) \quad (1)$$

Equal weight is given to each normalized (0 to 1) term such that the ranks range from 0 to 4, worst to best.

The statistical evaluation summarized in Table 1 produced several key findings. All three LPDMs seemed to perform well or poorly on the same experiments. For HYSPLIT and STILT there was at least one WRF-driven simulation for each experiment that was ranked higher than the NARR-driven simulation and for all but two of the experiments the NARR-driven simulation had the lowest rank. The best configuration for WRF included PBL wind nudging ($pb=1$) and the use of time-averaged fields (*avrg*) and for this combination there was little difference between the LPDMs with ranks ranging from 2.33 for FLEXPART to 2.42 for HYSPLIT. Nudging of PBL winds seemed to be beneficial to all LPDMs though slightly more so for FLEXPART. However, only HYSPLIT and STILT seemed to gain notable benefits from the use of time averaged fields and this is consistent with Brioude et al (2012) who found that using time-averaged velocities reduced the bias and uncertainty by less than 5% for FLEXPART simulations over complex terrain.

Table1. Average ranks over all tracer release experiments for HYSPLIT, STILT and FLEXPART for each type of meteorological input data.

	NARR ONLY	WRF			
		avrg		inst	
		pb=1	pb=0	pb=1	pb=0
HYSPLIT	2.13	2.42	2.34	2.29	2.29
STILT	2.12	2.39	2.26	2.26	2.27
FLEXPART		2.33	2.12	2.32	2.11

Case studies indicated that in the simulations without PBL wind nudging the plumes appeared to be transported too quickly away from the release locations. This overestimated transport speed may have resulted from a near-surface wind speed bias in WRF as reported by Jimenez and Dudhia (2012) that was partially corrected by nudging to NARR. The Case studies also revealed that the time-averaged fields produced smoother concentration patterns in HYSPLIT and STILT that were more consistent with observations.

Overall, the rigorous evaluation indicated that the meteorological input data were the dominant factor governing the accuracy of the transport simulations, rather than inter-model differences between the three LPDMs.

3. URBAN GHG SIMULATIONS

3.1 WRF-STILT Approach

STILT driven by customized WRF fields (WRF-STILT) underlies our top-down (inverse) approach for refining estimates of GHG emissions in urban areas. In our approach WRF-STILT is run backward-in-time from a set of receptors that are defined by the location and time of a measurement. The backward runs produce footprints that quantify the influence of upwind surface fluxes on concentrations measured at the receptors and are computed by counting the number of particles in a surface-influenced volume (defined as lower half of the PBL) and the time spent in that region (Lin et al. 2003). When multiplied by an *a priori* flux field ($\text{micromole m}^{-2} \text{s}^{-1}$), the footprint gives the associated contribution to the mixing ratio (ppmv) measured at the receptor. Adding this contribution to a background estimate provides a simulation of the GHG mixing ratio at the receptor. The simulated and measured mixing ratios can be compared and by applying various inverse techniques refinements to the *a priori* surface fluxes can be achieved.

A major uncertainty in GHG simulations is the ability of the meteorological model (WRF) to accurately represent the PBL throughout the diurnal cycle. The height of the PBL affects the depth to which surface emissions are mixed through turbulence and, along with the wind profile, impacts the rate at which emissions are transported away from their source. Typically, the PBL has a diurnal cycle of rapid growth and mixing in the morning followed by decay and stratification in the evening. Accurate PBL parameterizations and related surface physics are essential to robust GHG simulations and top-down flux estimates, as errors in the PBL height lead to proportional errors in the calculated concentrations at receptor locations (Lin et al. 2003). These errors can be especially pronounced for stable PBLs or during transitions to or from convective conditions. Since these transitions typically occur during the morning and evening hours, and since these periods also correspond to peak transportation emissions related to the daily commute in urban areas, these modeling errors can jeopardize the applicability of inverse modeling for monitoring long-term changes in emissions. To address these

uncertainties we focus on two urban areas, Salt Lake City (SLC) and Boston, which are distinct in their topographical and land-use characteristics.

3.2 Salt Lake City

The details of the Salt Lake City modeling study are provided in Nehrkorn et al. (2013) and only briefly summarized here. It was motivated by the existence of a multi-year CO₂ measurement network for a pilot study to determine the feasibility of using ground-based sensors to identify trends in anthropogenic urban emissions over time scales ranging from days to years. WRF ARW was run with high resolution (horizontal grid spacing ≤ 4 km) and a number sensitivity studies were performed with different PBL schemes and inner domain resolutions. The PBL schemes optionally included a single-layer urban canopy model (UCM; Chen et al. 2011) that accounted for the bulk effects of flow around buildings or “urban canopy” which is analogous to the vegetative canopy in forests. The WRF sensitivity runs were evaluated using profile data from the Vertical Transport and Mixing field-experiment (VTMX; Doran et al. 2002) in 2000.

The sensitivity runs indicated a clear benefit to using the UCM for simulating the PBL and near-surface conditions, particularly for temperature evolution at night as illustrated in Figure 1. When the UCM was used the boundary layer collapsed sooner after sunset closer to the observed timing and temperatures in urban areas were cooler and also closer to observations. The improvements due to the UCM were most notable during quiet synoptic conditions when flow was driven by local circulations but created little improvement during the active periods with synoptically driven flow.

The WRF sensitivity runs suggested that high-resolution meteorological models with a parameterization of the urban environment should be used for modeling the transport and dispersion of CO₂ in urban environments. This finding was confirmed by simulations for a 2-week period in October of 2006 for which complete WRF-STILT runs were conducted using both a lower-resolution 4-km grid without the UCM and a higher resolution (1.33 km) grid with the UCM WRF runs. The dynamic range of the simulated CO₂ for the 1.33km run with the UCM was closer to that of the observations. In addition the average diurnal cycle for the higher resolution UCM run was a better match to observations particularly in the early evening around time of the PBL collapse. These results suggest that high-resolution simulations with urban parameterization will

provide more robust top-down estimates of emissions trends in urban environments.

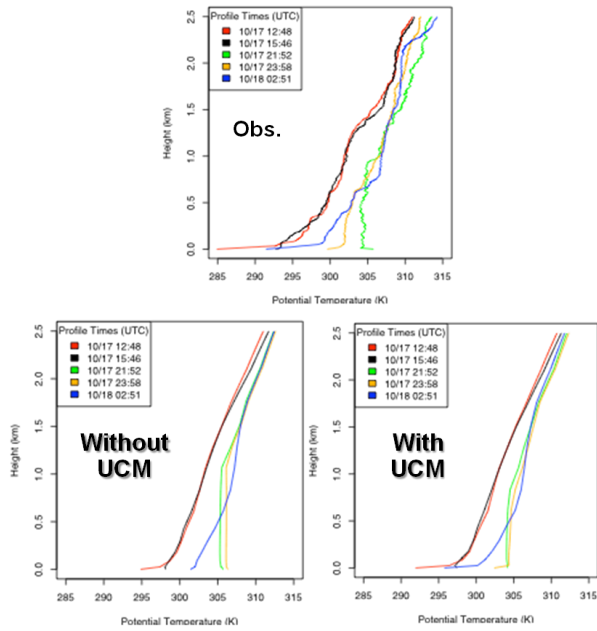


Fig 1. VTMX potential temperature profiles at different sounding times; observations (top center), WRF without UCM (bottom left), WRF with UCM (bottom right).

3.3 Boston

A project jointly funded by NASA, NSF and the Environmental Defense Fund (EDF) to characterize atmospheric CO₂ and CH₄ and monitor anthropogenic emissions trends in Boston and the surrounding metropolitan area is ongoing. The project supports long-term *in situ* measurements from several strategically placed towers and rooftop sites. This observing network makes several unique observations that include sampling from the 250 m level of the Prudential Tower (PRU), an isolated tall building located between Boston University (BU) and Boston Harbor. Complementing the *in situ* data, are remotely sensed total column measurements of CO₂, CH₄ and CO available from a Fourier Transform Spectrometer (FTS) and LiDAR aerosol profiles as a tracer of mixing. This suite of continuous ongoing measurements provides a robust data set for testing and optimizing WRF-STILT for monitoring GHG gas emissions in urban areas.

Following what was learned from the Salt Lake City study WRF is configured with a high resolution (1.33 km) inner domain centered on Boston and employs the UCM. Currently the simulations use WRF ARW version 3.4.1 and

initial and boundary conditions are provided by NARR. Simulations are restarted daily at 0000 UTC and run for 30 hours and the first 6 spin-up hours of each simulation are discarded.

Figure 2 shows a sample of the WRF-STILT CH₄ simulations for the BU and PRU sites for September - November 2012. The simulations seem to capture the overall diurnal cycle but there are still some timing issues particularly in the morning likely related to errors in the WRF PBL simulation.

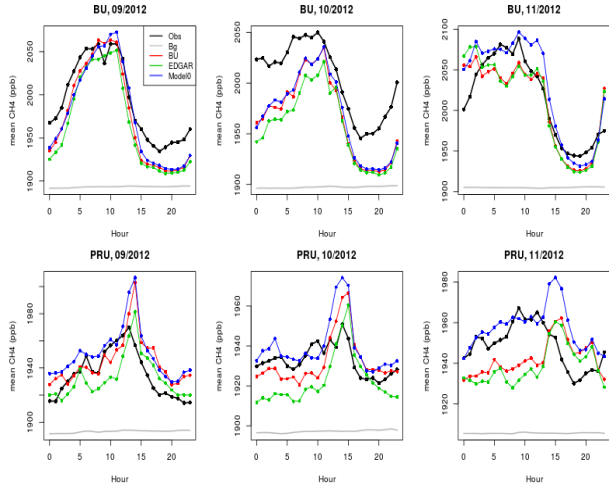


Fig. 2. Observed (black) and simulated (colored lines) average diurnal cycle of CH₄ mixing ratio at the BU and PRU sites for the months of September, October and November 2012; the hours are listed in UTC. The colored lines are for different emission inventories including a customized inventory from BU (red), EDGAR (green), and a uniform land source (blue). The background mixing ratio is in grey (from the coastal Nahant, MA site and Harvard Forest site west of Boston). The emissions were scaled up using a simple regression fit line for modeled versus observed mixing ratios.

One of the main goals of this modeling work is to minimize the errors in the GHG emissions estimates attributable to errors in the WRF PBL simulation. To accomplish this task we plan to make use of Mini Micro-Pulse LiDARs currently or soon to be deployed in Boston, Washington DC and New York City. The Mini Micro-Pulse LiDAR (MiniMPL) provides measurements of aerosol backscatter which can be used to infer PBL height. Sigma Space Corporation's Micro Pulse LiDAR (MPL, www.micropulselidar.com) provides continuous, unattended monitoring of atmospheric physical properties in real time including PBL height, vertical aerosol distribution and trends, cloud structure and phase, air pollution, dust, and volcanic ash. MPL systems have been produced

since 2004 under a license from NASA, and deployed in the NASA Micro-Pulse LiDAR NETWORK (MPLNET) and the US Department of Energy Atmospheric Radiation Measurement (ARM) program and other locations worldwide. MiniMPL is an innovation improving portability and power efficiency and lowering cost, while maintaining the high signal-to-noise ratio of many laboratory-class LiDARs and Class II eye safety. MiniMPL measurements of PBL height generally compare well with independent data, as shown in Figure 3.

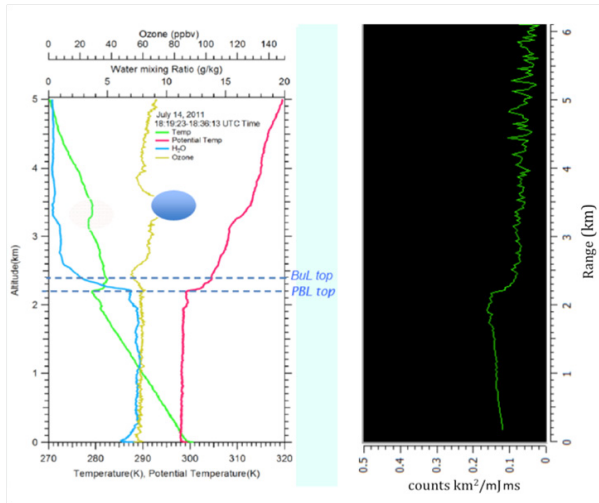


Fig. 3. Data from balloon sondes (left) and Sigma Space Mini MPL Normalized Relative Backscatter (NRB) profile (right) collected during the NASA DISCOVER-AQ mission on July 14th, 2011, 18:40 UTC in Edgewood, MD. The MiniMPL profile is a single 30-second integration time profile with 30-meter range bins. Both data sets show a PBL top at circa 2.2 km and the presence of a shallow buffer layer between the boundary layer and the free troposphere.

MiniMPL measurements of PBL heights are a key component in a growing number of urban GHG flux studies, with a pilot deployment during the 2012 World Economic Forum in Davos, Switzerland (Lauvaux et al. 2013) and sustained deployments in Boston and as part of the Los Angeles Megacity project. For example the measured aerosol backscatter for July 16, 2012 at BU shows the diurnal cycle of growth and decay of the PBL (Figure 4). The WRF PBL simulation generally matches that observed by the Mini-MPL during the day, but underestimates the PBL depth during the night and early morning hours. Also, the WRF PBL collapses too quickly during the evening. By evaluating the WRF simulations with these types of comparisons it may be possible to optimize WRF by selecting the best combination of

PBL and other physics options for the Boston area. Alternatively, and in conjunction with this optimization, the MiniMPL measurements will help us eliminate from our top-down inversion those time periods in which the WRF simulation errors of the PBL are unacceptably large. By comparing emissions estimates with and without these time periods we will be able to more precisely quantify the impact of these errors on top-down estimates of emission trends.

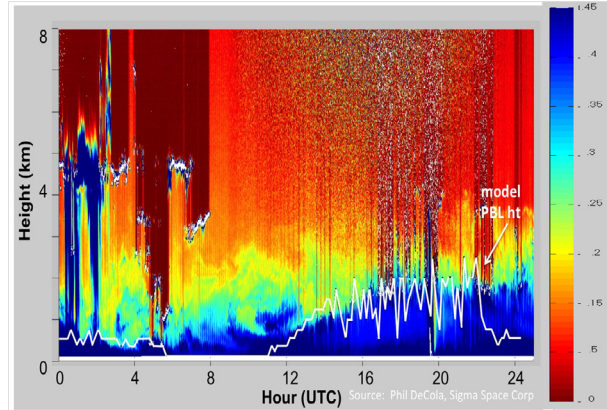


Fig. 4. Time series of MiniMPL backscatter (color field) during deployment on the BU rooftop on July 16, 2012. The time series shows scattered low and mid-level clouds (white on color scale) on the left above the residual boundary layer (yellow and green) with embedded dynamical features of the nocturnal PBL and at the PBL top followed by the growth of the daytime PBL (blue). The WRF simulated PBL height is shown as a solid white line.

4. SUMMARY

Through a rigorous statistical evaluation using controlled tracer data we have shown that three current LPDMs perform equally provided with identical meteorological inputs and that these inputs were the dominant factor governing the accuracy of the tracer simulations. The application of WRF-STILT to GHG simulations in urban areas was shown to benefit from improved spatial resolution and the use of an urban canopy model in WRF. An ongoing study in Boston with an extensive network of *in situ* and remotely sensed measurements and the deployment of MiniMPLs is expected to provide a robust dataset for evaluating and optimizing high resolution WRF-STILT simulations for monitoring trends in urban emissions. While these past and ongoing studies most directly relate to a Lagrangian modeling framework, the strong dependence on the

meteorological inputs suggests that their findings should be applicable to many different types of air quality model simulations.

6. REFERENCES

- Brioude, J., W. M. Angevine, S. A. McKeen, and E.-Y. Hsie, 2012: Numerical uncertainty at mesoscale in a Lagrangian model in complex terrain. *Geosci. Model Dev.*, **5**, 1127–1136.
- Chen, F., and Coauthors, 2011: The integrated WRF/urban modeling system: Development, evaluation, and applications to urban environmental problems. *Int. J. Climatol.*, **31**, 273–288.
- Doran, J. C., J. D. Fast, and J. Horel, 2002: The VTMX 2000 campaign. *Bull. Amer. Meteor. Soc.*, **83**, 537–551.
- Draxler, R. R., 2006: The Use of Global and Mesoscale Meteorological Model Data to Predict the Transport and Dispersion of Tracer Plumes over Washington, D.C. *Wea. Forecasting*, **21**, 383–394.
- Draxler, R. R., and G. D. Hess, 1998: An overview of the HYSPLIT₄ modelling system for trajectories, dispersion, and deposition. *Aust. Meteor. Mag.*, **47**, 295–308.
- Draxler, R. R., and J. L. Heffter, 1989: *Across North America Tracer Experiment (ANATEX) Volume I: Description, Ground-Level Sampling at Primary Sites, and Meteorology, January*, NOAA Tech Memo ERL ARL-167. Air Resources Laboratory, Silver Spring, MD, 83 pp.
- Eluszkiewicz, J., R. S. Hemler, J. D. Mahlman, L. Bruhwiler, and L. L. Takacs, 2000: Sensitivity of age-of-air calculations to the choice of advection scheme. *J. Atmos. Sci.*, **57**, 3185–3201.
- Ferber, G. J., J. L. Heffter, R. R. Draxler, R. J. Lagomarsino, F. L. Thomas, and R. N. Dietz, 1986: *Cross-Appalachian Tracer Experiment (CAPTEX '83) Final Report*, NOAA Tech Memo ERL ARL-142. Air Resources Laboratory, Silver Spring, MD, 60 pp.
- Hegarty, J. D., R. R. Draxler, A. F. Stein, J. Brioude, M. Mountain, J. Eluszkiewicz, T. Nehrkorn, F. Ngan, and A. E. Andrews, Evaluation of lagrangian particle dispersion models from controlled tracer releases, *J. Appl. Meteorol. Climatol.*, in press.
- Jiménez, P. A., and J. Dudhia, 2012: Improving the representation of resolved and unresolved topographic effects on surface wind in the WRF model. *J. Appl. Meteor. Climatol.*, **51**, 300–316.
- Lauvaux, T., N. Miles, S. Richardson, A. Deng, D. Stauffer, K. Davis, G. Jacobson, C. Rella, P. DeCola, and G-P. Calonder, 2013: Urban emissions of CO₂ from Davos, Switzerland: the first real-time monitoring system using an atmospheric inversion technique. *J. Appl. Meteorol. Climatol.* doi:10.1175/JAMC-D-13-038.1, in press.
- Lin, J. C., C. Gerbig, S. C. Wofsy, B. C. Daube, A. E. Andrews, K. J. Davis, and C. A. Grainger, 2003: A near-field tool for simulating the upstream influence of atmospheric observations: the stochastic time-inverted lagrangian transport (STILT) model. *J. Geophys. Res.*, **108** (D16):4493. doi:10.1029/2002JD003161.
- Mesinger, F. and Coauthors, 2006: North American Regional Reanalysis. *Bull. Amer. Meteor. Soc.*, **87**, 343–360.
- Mosca, S., G. Graziani, W. Klug, R. Bellasio, and R. Bianconi, 1998: A statistical methodology for the evaluation of long-range dispersion models: An application to the ETEX exercise. *Atmos. Environ.*, **32**, 4307–4324.
- Nehrkorn, T., J. Eluszkiewicz, S. C. Wofsy, J. C. Lin, C. Gerbig, M. Longo, and S. Freitas, 2010: Coupled Weather Research and Forecasting-Stochastic Time-Inverted Lagrangian Transport (WRF-STILT) model. *Meteor. Atmos. Phys.*, **107**, 51–64.
- Nehrkorn, T., J. Henderson, M. Leidner, M. Mountain, J. Eluszkiewicz, K. McKain, and S. Wofsy, 2013: WRF simulations of the urban circulation in the Salt Lake City area for CO₂ modeling. *J. Appl. Meteorol. Climatol.*, **52**, 323–340.
- Skamarock, W. C., and J. B. Klemp, 2008: A time-split nonhydrostatic atmospheric model for weather research and forecasting applications. *J. Comp. Phys.*, **227**, 3465–3485.
- Stohl, A., M. Hittenberger, and G. Wotawa, 1998: Validation of the Lagrangian particle dispersion model FLEXPART against large-scale tracer experiment data. *Atmos. Environ.*, **32**, 4245–4264.
- Stohl, A., C. Forster, A. Frank, P. Seibert, and G. Wotawa, 2005: Technical note: The Lagrangian particle dispersion model FLEXPART version 6.2. *Atmos. Chem. Phys.*, **5**, 2461–2474.

ACKNOWLEDGMENTS

Support for this study is from the National Science Foundation (grants ATM-0836153, ATM-1207983 and ATM-1302902) and NOAA (grants WE133R11SE2312 and RA-133R-12-SE-2198).